4H05 Development of a thermal vacuum testing system using Peltier element

Joseph Ampadu OFOSU, Hirokazu MASUI, and Mengu CHO
Center for Nanosatellite Testing, Kyushu Institute of Technology, Kitakyushu 804-8550, Japan

Key Words: Thermal Vacuum Testing, Thermal Balance, Thermal Cycle, CubeSat

Abstract

The concept of lean satellites is driving academia, industry, and governments across the globe to pursue space for research and education, economics, technological demonstration, security and many more. An objective of this concept is making space accessible, affordable, and reliable, especially for new entrants in the space field. One of the ways to achieve this is making environmental testing of satellites accessible and inexpensive. We present in this paper, the development of a comparatively inexpensive thermal vacuum testing system, equipped with a thermoelectric device that uses the Peltier principle of heat generation. The thermoelectric device is a commercial-off-the-shelf (COTS) component with a cooling capacity of 16.9 W. The testing system does not require LN_2 or silicon oil for simulating cold conditions. In addition, the testing system is capable of vacuum thermal cycling and balancing tests within -45 ℃ to +75 ℃, well beyond the minimum requirements of the ISO-19683. These characteristics make the testing system simple, accessible, and inexpensive. We hope that this testing system would foster the growth of scientific and technical endeavors within the CubeSat community.

1. Introduction

Thermoelectric modules (TEMs) are solid-state devices that utilize thermoelectric effects for energy conversion between thermal and electrical forms. The effects which include Seebeck, Peltier and Thomson, together with the principles of Joule heating and Fourier conduction have been known approximately for the past 2 centuries.[1] The advent and advances in semiconductor technology,[2]–[4] the potential applications and the attractive features of TEMs have focused lots of research efforts in recent years on thermoelectric devices. Some features of TEMs include compact in size, clean with no moveable parts hence simple and maintenance-free, no requirements for refrigerants, have high energy density, adaptable and environmentally friendly.[2], [5]–[7] TEMs are grouped as (1) thermoelectric coolers (TECs) which are used for cooling/ heating applications and (2) thermoelectric generators (TEGs) for electricity generation from temperature gradients.[8]–[10] TEC applications include thermal management of optical devices such as lasers, intensified charge coupled devices, and processing units of computational devices. TEG applications include electricity generation in space missions, thermocouple sensors, and waste heat harvesting from the exhaust of automobiles.[11]–[15] A demerit for TEMs especially TEG devices is their low energy conversion efficiency which limits applications to low power systems and thus economically non-viable compared with conventional energy generators.[16], [17] Nonetheless, numerous research efforts via analytical,[18]–[21] numerical simulation[22]–[25] and experimental studies[26]–[30] are being carried out to improve the thermoelectric conversion efficiency of TEMs.

The number of smallsats launches have been on the rise in recent years, and as indicated by BryceTech, the year 2020 received 40% of all smallsats launched in the past 10 years. Of the 1202 smallsats launched in 2020, 11% and 3% were respectively for remote sensing and technology development.[31] Most of these were of the Nano and Micro satellite categories. With Kyushu Institute of Technology as the academic institute with the largest number of satellites launched in the past 10 years, we at the Center for Nanosatellite Testing (CeNT) are working toward the objective of making space accessible, affordable, and reliable for new entrants in the space field.

In this paper we present the progress of ongoing work on an inexpensive thermal vacuum testing (TVT) system at CeNT. This TVT system which has been used in testing an engineering model of a 1U CubeSat does not require the

supply of liquid nitrogen (LN_2) for cooling and has been extensively described in reference [32]. The TVT system uses a TEM for both cooling and heating based on the Peltier effect principle. In the following sections, we present the thermal unit of the TVT, no-load and load conditions tests and comparison of performance parameters.

2. The thermal unit

The thermal unit schematically shown in Fig. 1 comprises two 4-stage Peltier element sandwiched between a copper (Cu) shroud plate and an aluminum (Al) heat sink. A compressible thermal gap filler for minimizing contact thermal resistance is interfaced between the elements at the top with the Cu plate and at the bottom with the Al heatsink. The heatsink is equipped with Cu piping for effective heat dissipation. The entire unit is isolated from the chamber wall using 4 PTFE support bases as shown in Fig. 2.

The shroud part of the thermal unit which holds test articles, is made up of the Cu plate and a Cu sheet; thermally insulated from each other by a room-temperature-vulcanizing (RTV) adhesive. The internal part of the shroud is black coated to increase radiative emissivity and absorptivity. The entire shroud is covered with a multi-layer insulation (MLI) material to minimize heat losses as the chamber is always at room temperature conditions. PTFE spacers are used to support the weight of the Cu shroud and serve as thermal isolators between the

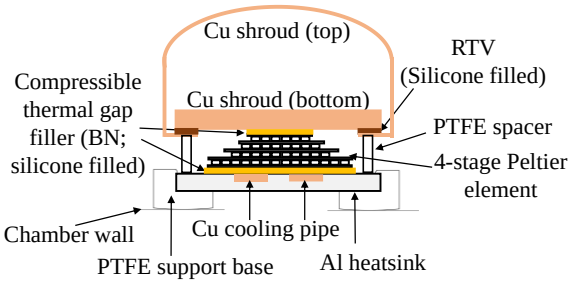

Fig.1. Schematic representation of the thermal unit.

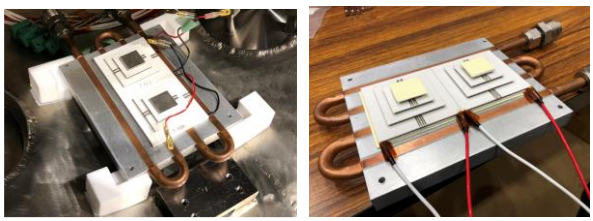

Fig. 2. Pictures of the Peltier elements, Al heatsink, PTFE blocks and thermal gap filler

Cu shroud and the Al heatsink. Heat dissipation from the Al heatsink is achieved by circulating coolant/fluid at a maximum flow rate of 20 liters/ minute. Table 1 shows the physical, thermal, and electrical properties of some components of the thermal unit.

Table 1. Thermal unit components' properties.

4-stage Peltier element	
Manufacturer	Kryotherm
Module name	TB-4-(199-97-49-17)-1.5
Maximum current, A	6.7
Maximum voltage, V	23.6
Max temp. difference, ℃ (or K)	111
AC resistance, Ω	3.42
Operating temperature, ℃	-50 - +80
Thermal gap filler	
Manufacturer	Laird Technologies
Model number	TPLI 240
Composition	Boron nitride with silicone
Thickness, mm	1.02
Density, g/ cc	1.43
Outgassing CVCM, %	0.02
Operating temperature, ℃	-45 - +200
Thermal conductivity, (W/ mK)	6
AC Breakdown voltage, V	> 5000
Room-temperature-vulcanizing adhesive	
Manufacturer	Wacker-Chemie GmbH
Model number	RTV S 691
Specific gravity	1.41 – 1.43
Thermal conductivity, (W/ m℃)	0.39
Operating temperature, ℃	-180 - +200
Circulator and coolant	
Manufacture, Model	Axel, LTC1200a
Circulator capacity, L	16
Max. flow rate, L/ min	20
Operating temperature, ℃	-20 - +30
Coolant	Ethylene glycol (90-94 wt%)
Coolant: deionized water mix. ratio	0.4:0.6

3. Thermal vacuum test runs

Test runs were conducted using the thermal unit configuration of Fig. 1 at both no-load and load conditions. The Peltier elements were operated at approximately 33% of their current and voltage ratings; respectively 2 A and 8 V. In order to achieve a minimum coolant temperature of -25 ℃, the mixture ratio of coolant to deionized water was set as 0.4:0.6. Figure 3 shows the temperature and pressure profiles of the no-load test conducted for about 32 hours. Two cycles were performed with a dwell time in the first cycle at an approximately 2 hours. This is very typical for the dwell times for vacuum thermal cycling tests of CubeSats. The dwell time for the second cycle was about 8 hours, which is typical for the vacuum thermal balance

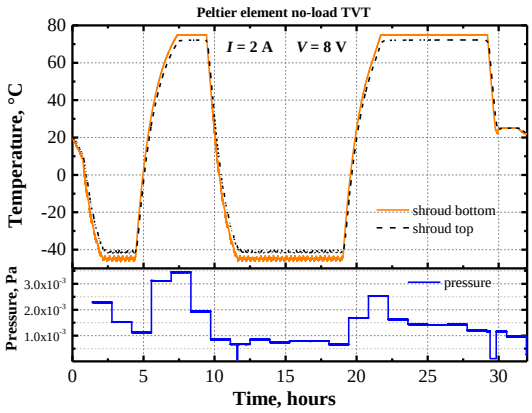

Fig. 3. Temperature and pressure profiles of the Peltier element no-load TVT.

tests of satellites. For heating applications, the polarity of the Peltier elements was reversed using the same current voltage levels.

We observe that the worst cold and hot case temperatures were -45 ℃ and +75 ℃ respectively for the Cu shroud plate, well beyond the minimum requirements of the ISO-19683 standard. The temperature difference between the shroud bottom and the shroud top was about 5 ℃ during the entire test. This shows that radiative heating/ cooling was efficient because, both the shroud bottom and top were thermally isolated. During cooling, the top part of Peltier element transfers heat to the bottom whiles the reverse action occurs when heating. To avoid exceeding the maximum temperature difference between the hot and cold side plates of the Peltier element (i.e. 111 K), the coolant temperature was set to -15 ℃ and +25 ℃ during cooling and heating respectively.

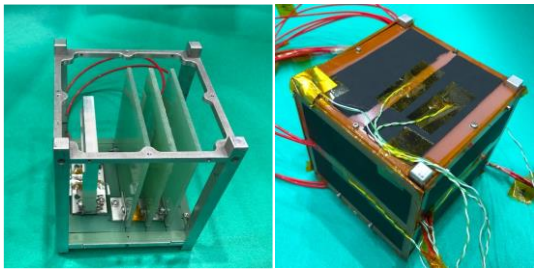

Fig. 4. 1U dummy CubeSat used for the TVT test runs

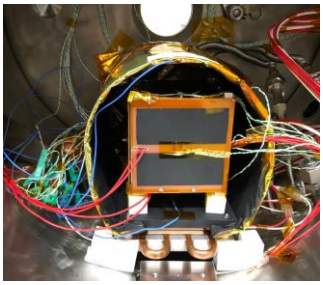

Fig. 5. Dummy CubeSat in shroud isolated by PTFE blocks from the shroud bottom plate.

Figures 4 and 5 show the 1U dummy CubeSat used for the TVT test run. The mass of the satellite was approximately 750 g. The temperature profiles of the test are shown in Fig. 6 for a continuous test period of 74 hours for 2.5 thermal cycles. The satellite temperatures are represented by the panels, Al frame, internal Al blocks and epoxy glass slabs. The satellite attained worst cold and hot case temperatures of -38 ℃ and +70 ℃ respectively, when that of the shroud was limited to -45 ℃ and +75 ℃. This indicates an efficient transfer of heat during the entire test duration. The ramp rate for the entire test was approximately ±0.5 ℃/ min. For a perspective, the ramp rate was similar to that of our small and big chambers at CeNT. However, the ramp rate for heating was about half that of our heaters for environmental testing of satellites.

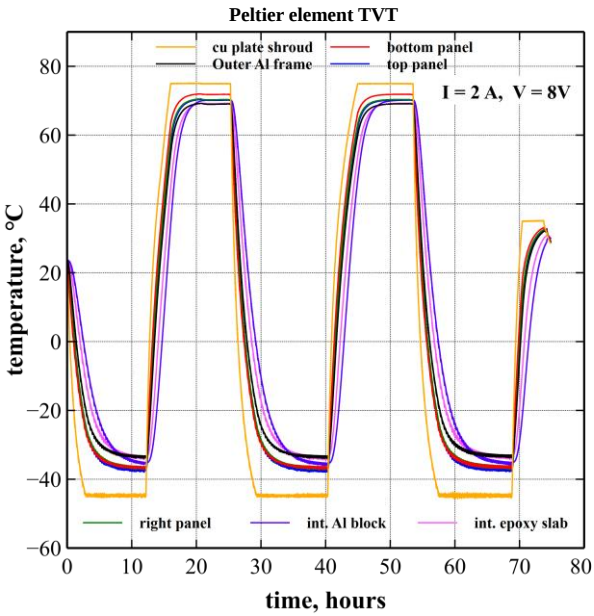

Fig. 6. Temperature profiles of the Peltier element TVT.

Comparatively, a typical 2-cycle TVT test of a 1U CubeSat at CeNT, requires about 2 kPa usage of LN_2 supply. This is costed as 20,400 JPY (2 kPa × 136 kg/ kPa × 75 JPY/ kg) and is equivalent to a unit cost of the 4-stage TEM (US$ 225) used in this study. More so, a typical test would require at least 4 DC power supplies compared to just 1 used in this study. Thus, the running cost comparison evidently shows that the TEM device is a cost-effective option compared to the conventional way of testing, without even considering the equipment cost for LN_2.

4. Summary

In this study, we have demonstrated the applicability of a TEM based on the principle of Peltier effect to thermal vacuum testing of a 1U CubeSat. Using two 4-stage Peltier element, and running them at 33% of their electrical ratings, temperatures within -45 ℃ to +75 ℃ were attained, well beyond the minimum requirements of the ISO-19683. These make the testing system simple, accessible, and inexpensive. We intend to further improve the system performance of this test device and hope that it would facilitate the growth of scientific, and technical endeavors within the CubeSat community.

References

[1] H. J. Goldsmid, "The Thermoelectric and Related Effects," *Springer Series in Materials Science*, vol. 121, pp. 1–6, 2010, doi: 10.1007/978-3-642-00716-3_1.

[2] D. M. Rowe, Ed., *Thermoelectrics Handbook*, 1st ed. CRC Press, 2018. doi: 10.1201/9781420038903.

[3] H. J. Goldsmid and R. W. Douglas, "The use of semiconductors in thermoelectric refrigeration," *British Journal of Applied Physics*, vol. 5, no. 11, pp. 386–390, Nov. 1954, doi: 10.1088/0508-3443/5/11/303.

[4] L. D. Hicks and M. S. Dresselhaus, "Thermoelectric figure of merit of a one-dimensional conductor," *Physical Review B*, vol. 47, no. 24, pp. 16631–16634, 1993, doi: 10.1103/PhysRevB.47.16631.

[5] M. Zebarjadi, K. Esfarjani, M. S. Dresselhaus, Z. F. Ren, and G. Chen, "Perspectives on thermoelectrics: From fundamentals to device applications," *Energy and Environmental Science*, vol. 5, no. 1, pp. 5147–5162, Jan. 2012, doi: 10.1039/c1ee02497c.

[6] F. J. Disalvo, "Thermoelectric cooling and power generation," *Science*, vol. 285, no. 5428, pp. 703–706, Jul. 1999, doi: 10.1126/science.285.5428.703.

[7] S. B. Riffat and X. Ma, "Thermoelectrics: A review of present and potential applications," *Applied Thermal Engineering*, vol. 23, no. 8, pp. 913–935, Jun. 2003, doi: 10.1016/S1359-4311(03)00012-7.

[8] A. F. Ioffe, L. S. Stil'bans, E. K. Iordanishvili, T. S. Stavitskaya, A. Gelbtuch, and G. Vineyard, "Semiconductor Thermoelements and Thermoelectric Cooling," *Physics Today*, vol. 12, no. 5, p. 42, Jan. 1959, doi: 10.1063/1.3060810.

[9] S. Wen, G. Zhang, Y. Dan, D. Wang, and M. Deng, "Model output following control for an aluminum plate cooling process with a Peltier device," Sep. 2012. Accessed: Sep. 02, 2021. [Online]. Available: https://ieeexplore.ieee.org/document/6329622

[10] C. C. Wang, C. I. Hung, and W. H. Chen, "Design of heat sink for improving the performance of thermoelectric generator using two-stage optimization," *Energy*, vol. 39, no. 1, pp. 236–245, Mar. 2012, doi: 10.1016/J.ENERGY.2012.01.025.

[11] A. Basti, T. Obikawa, and J. Shinozuka, "Tools with built-in thin film thermocouple sensors for monitoring cutting temperature," *International Journal of Machine Tools and Manufacture*, vol. 47, no. 5, pp. 793–798, Apr. 2007, doi: 10.1016/J.IJMACHTOOLS.2006.09.007.

[12] M. S. El-Genk, H. H. Saber, and T. Caillat, "Efficient segmented thermoelectric unicouples for space power applications," *Energy Conversion and Management*, vol. 44, no. 11, pp. 1755–1772, Jul. 2003, doi: 10.1016/S0196-8904(02)00217-0.

[13] D. Samson, M. Kluge, T. Fuss, U. Schmid, and Th. Becker, "Flight Test Results of a Thermoelectric Energy Harvester for Aircraft," *Journal of Electronic Materials 2012 41:6*, vol. 41, no. 6, pp. 1134–1137, Feb. 2012, doi: 10.1007/S11664-012-1928-6.

[14] J. P. Longtin *et al.*, "Fabrication of Thermoelectric Devices Using Thermal Spray: Application to Vehicle Exhaust Systems," *Journal of Thermal Spray Technology 2013 22:5*, vol. 22, no. 5, pp. 577–587, Feb. 2013, doi: 10.1007/S11666-013-9903-1.

[15] C. Lu, S. Wang, C. Chen, and Y. Li, "Effects of heat enhancement for exhaust heat exchanger on the performance of thermoelectric generator," *Applied Thermal Engineering*, vol. 89, pp. 270–279, Oct. 2015, doi: 10.1016/J.APPLTHERMALENG.2015.05.086.

[16] T. C. Harman, M. P. Walsh, B. E. laforge, and G. W. Turner, "Nanostructured thermoelectric materials," *Journal of Electronic Materials 2005 34:5*, vol. 34, no. 5, pp. L19–L22, 2005, doi: 10.1007/S11664-005-0083-8.

[17] C. B. Vining, "An inconvenient truth about thermoelectrics," *Nature Materials 2009 8:2*, vol. 8, no. 2, pp. 83–85, 2009, doi: 10.1038/nmat2361.

[18] S. Lineykin and S. Ben-Yaakov, "Modeling and analysis of thermoelectric modules," *IEEE Transactions on Industry Applications*, vol. 43, no. 2, pp. 505–512, 2007, doi: 10.1109/TIA.2006.889813.

[19] Y. Wu, L. Zuo, J. Chen, and J. A. Klein, "A model to analyze

the device level performance of thermoelectric generator," *Energy*, vol. 115, pp. 591–603, 2016, doi: 10.1016/j.energy.2016.09.044.

[20] R. Bjørk, D. v. Christensen, D. Eriksen, and N. Pryds, "Analysis of the internal heat losses in a thermoelectric generator," *International Journal of Thermal Sciences*, vol. 85, pp. 12–20, 2014, doi: 10.1016/j.ijthermalsci.2014.06.003.

[21] R. Shen, X. Gou, H. Xu, and K. Qiu, "Dynamic performance analysis of a cascaded thermoelectric generator," *Applied Energy*, vol. 203, pp. 808–815, 2017, doi: 10.1016/j.apenergy.2017.06.108.

[22] E. Fang, X. Wu, Y. Yu, and J. Xiu, "Numerical modeling of the thermoelectric cooler with a complementary equation for heat circulation in air gaps," *Open Physics*, vol. 15, no. 1, pp. 27–34, 2017, doi: 10.1515/phys-2017-0004.

[23] S. Manikandan and S. C. Kaushik, "The influence of Thomson effect in the performance optimization of a two stage thermoelectric generator," *Energy*, vol. 100, pp. 227–237, 2016, doi: 10.1016/j.energy.2016.01.092.

[24] F. Meng, L. Chen, and F. Sun, "A numerical model and comparative investigation of a thermoelectric generator with multi-irreversibilities," *Energy*, vol. 36, no. 5, pp. 3513–3522, 2011, doi: 10.1016/j.energy.2011.03.057.

[25] O. Högblom and R. Andersson, "A simulation framework for prediction of thermoelectric generator system performance," *Applied Energy*, vol. 180, pp. 472–482, 2016, doi: 10.1016/j.apenergy.2016.08.019.

[26] S. Wang, T. Xie, and H. Xie, "Experimental study of the effects of the thermal contact resistance on the performance of thermoelectric generator," *Applied Thermal Engineering*, vol. 130, pp. 847–853, 2018, doi: 10.1016/j.applthermaleng.2017.11.036.

[27] R. Bjørk, A. Sarhadi, N. Pryds, N. Lindeburg, and P. Viereck, "A thermoelectric power generating heat exchanger: Part i - Experimental realization," *Energy Conversion and Management*, vol. 119, pp. 473–480, 2016, doi: 10.1016/j.enconman.2016.04.042.

[28] X. Liang, X. Sun, H. Tian, G. Shu, Y. Wang, and X. Wang, "Comparison and parameter optimization of a two-stage thermoelectric generator using high temperature exhaust of internal combustion engine," *Applied Energy*, vol. 130, pp. 190–199, 2014, doi: 10.1016/j.apenergy.2014.05.048.

[29] C. Amaral, C. Brandão, É. v. Sempels, and F. J. Lesage, "Net thermoelectric generator power output using inner channel geometries with alternating flow impeding panels," *Applied Thermal Engineering*, vol. 65, no. 1–2, pp. 94–101, 2014, doi: 10.1016/j.applthermaleng.2013.12.044.

[30] C. T. Hsu, G. Y. Huang, H. S. Chu, B. Yu, and D. J. Yao, "Experiments and simulations on low-temperature waste heat harvesting system by thermoelectric power generators," *Applied Energy*, vol. 88, no. 4, pp. 1291–1297, 2011, doi: 10.1016/j.apenergy.2010.10.005.

[31] BryceTech, "Smallsats by the Numbers," 2021.

[32] B. Bonsu, H. Masui, and M. Cho, "Peltier-based Thermal Testing (PeTT) Vacuum Chamber: Affordable Testing Facility for Lean Satellites," *UNISEC Space Takumi*, vol. 8, no. 2, pp. 11–38, 2019.